JOURNAL OF MATERIALS SCIENCE 22 (1987) 2369–2376

Preparation and characterization of binary V_2O_5–Bi_2O_3 glasses

ASWINI GHOSH, B. K. CHAUDHURI
Department of Magnetism, Indian Association for the Cultivation of Science, Jadavpur, Calcutta 700 032, India

Characterization of the binary V_2O_5–Bi_2O_3 glasses prepared by rapidly quenching the melt has been made from the studies of X-ray diffraction, scanning electron microscopy, infrared absorption, differential thermal analysis, electron paramagnetic resonance, chemical analysis, density and electrical properties. Stable glasses are obtained for 95 to 75 mol% V_2O_5 by quenching on a stainless steel substrate, while quenching on a copper substrate extends the glass formation range from 95 to 70 mol% V_2O_5. The V–O bond vibration in the glasses occurs at 1020 cm^{-1} and the V^{5+} ion exists in six-fold coordination as in crystalline V_2O_5. All the glasses appear to be in single phase. The spin concentration in the glasses is found to be independent of temperature. A second heat-treatment at 255° C develops crystalline phase in the glasses. Unlike infrared absorption, electron paramagnetic resonance, density and chemical compositions, the electrical and thermal (DTA) properties are found to be slightly sensitive to the thermal history of preparation of the glasses. The high-temperature (300 to 500 K) conduction in the glasses seems to be due to adiabatic hopping of polarons. The thermopower is observed to be independent of temperature and provides evidence for small polaron formation in the glasses.

1. Introduction

Transition metal oxides such as V_2O_5, MoO_3, etc., when heated with glass-forming oxides like P_2O_5, TeO_2, etc., from glasses on quenching the melt [1–3]. These glasses are important because of their semiconducting properties. The electrical conduction in them is due to the hopping of electrons (or polarons) on account of available reduced states of the transition metal ions [4–7]. The vandate glasses have been studied extensively with the glass former P_2O_5 [5, 7]. Investigations of electrical conduction [4–9], dielectric relaxation [10, 11] and spectroscopic studies [12] of these glasses have been reported. The effect of single [13, 14] and multiple [15, 16] transition metal ions as dopants in alkali or alkaline earth oxide glasses has also been studied. In order to throw more light on the structural and electronic properties of transition metal oxide glasses, it is necessary to study these glasses with other glass formers such as Bi_2O_3, TeO_2, etc. Although, Heynes and Rawson [17] have only reported the formation of V_2O_5–Bi_2O_3 glasses in the rather narrow composition range 90.5 to 82.5 mol% V_2O_5, characterizations of these V_2O_5–Bi_2O_3 glasses have not yet been reported in the literature. Therefore, these V_2O_5–Bi_2O_3 glasses have been prepared by quenching on different substrates (copper and stainless steel) and characterized from the studies of X-ray diffraction, scanning electron microscopy, infrared absorption, differential thermal analysis (DTA), electron paramagnetic resonance (EPR), density and high-temperature electrical properties. The glass formation range in the V_2O_5–Bi_2O_3 glasses has also been extended from 95 to 70 mol% V_2O_5 in the present work.

2. Experimental details

2.1. Glass preparation

The glass samples were prepared from analar grade V_2O_5 (Reanal, Hungary) and Bi_2O_3 (E. Merck, Germany). The weighed quantities of these chemicals in appropriate proportions were thoroughly mixed. The starting compositions were from 95 to 65 mol% V_2O_5 at intervals of 5 mol%. The mixture was placed in a quartz (or platinum) crucible and melted in an electrical furnace. The melt was held at a temperature of 900° C for 2 h and was shaken frequently to ensure proper mixing and homogeneity. The melt was then poured on to an ice-cooled stainless steel block and was immediately pressed by another stainless steel block (steel block quenching or SBQ). The glasses were also prepared using two polished copper blocks instead of steel blocks (copper block quenching, or CBQ). The pressed samples were between 0.5 and 1.0 mm thick and were dark black in colour. The samples were washed with analar grade benzene and polished with very fine lapping papers. The X-ray diffraction showed that good glasses were obtained for 95 to 75 mol% V_2O_5 content by the SBQ technique, while good glasses were formed with 95 to 70 mol% V_2O_5 by the CBQ technique. Partial crystallinity was observed in the samples with V_2O_5 content up to 65 mol% prepared by both techniques.

Samples of different compositions prepared by these techniques at different times also showed reproducible results. The characteristic features of the glasses prepared in quartz as well as in platinum crucibles were found to be similar, indicating that the container in which the sample was melted had no effect on the

0022–2461/87 $03.00 + .12

amorphous character of the prepared samples. The results for the glasses prepared in platinum crucibles are reported in this paper.

2.2. Measurements

2.2.1. *X-ray diffraction*

X-ray diffraction of the powdered samples of all the prepared glasses was taken using an X-ray generator and recorder system (Philips PW 1050/51 coupled with PW 1130 generator) for their structures. The starting materials V_2O_5 and Bi_2O_3 were also subjected to X-ray diffraction under identical experimental conditions, for comparison. The samples were also tested for their amorphous structures after annealing at 200° C (well below the glass transition temperature as determined by DTA) for 2 h. The same samples were also tested after a second heat-treatment at 255° C.

2.2.2. *Scanning electron microscopy (SEM)*

Scanning electron micrographs were taken of the surfaces of the polished samples etched with 1% HCl for 1 min using a Hitachi (Japan), model S-415A scanning electron microscope. A 20 nm thick gold coating was deposited on the polished surfaces by vacuum evaporation to serve as the conduction layer.

2.2.3. *Infrared spectra*

The infrared absorption spectra of the prepared glasses and the starting materials V_2O_5 and Bi_2O_3 in KBr matrix were recorded on a Perkin–Elmer Spectrophotometer, model 783 at room temperature. The powdered samples were thoroughly mixed with dry KBr in the ratio 1 : 50 and then pellets were formed in an evacuable dye at 60% relative humidity. The pellets were clear and uniform. While recording the spectra, the gain of the spectrometer was kept the same for all the samples.

2.2.4. *Differential thermal analysis (DTA)*

The differential thermal analysis was performed for all the samples using a Shimadzu DT-30 thermal analyser with a heating rate of $20^\circ \mathrm{C\,min^{-1}}$.

2.2.5. *Density*

The densities of the glass samples were measured at room temperature by the displacement method using benzene as the immersion liquid and a single pan balance of 10^{-4} g sensitivity.

2.2.6. *EPR spectra*

The EPR spectra of the powdered glasses were taken using a Varian E-12 X-band EPR spectrometer at different temperatures. The concentrations of V^{4+} ions were estimated from the spectra using a single crystal of copper sulphate pentahydrate as a standard.

2.2.7. *Chemical compositions*

The final chemical compositions of all the samples and the concentrations of V^{4+} and V^{5+} ions were determined by redox-titration of the solutions of the samples in dilute HCl against potassium permanganate solution [18]. Standard chemical analysis was also performed for the glasses prepared in quartz crucibles to detect any trace of silica suspected to be dissolved in the melt from the crucible, but no trace of silica was detected.

2.2.8. *Electrical measurement*

For electrical measurements, disc-shaped samples of diameter ~8 mm and thickness 0.5 to 1.0 mm were cut and polished with very fine lapping papers. Gold electrodes were deposited on both faces of the samples by a sputtering technique. The samples were annealed at 200° C for 2 h to stabilize the gold contacts. Finally, ohmic contacts were checked by drawing *I–V* characteristics. The d.c. conductivity of the samples was measured in the temperature range 300 to 500 K using a Keithley 640 Vibrating Capacitor Electrometer. The conductivity of the samples of the same compositions from different batches agreed within a factor of two. Thermopowers of the samples were measured in the temperature range 300 to 500 K.

3. Results and discussion

3.1. X-ray diffraction and glass formation

The X-ray diffractograms of the powdered samples of the prepared V_2O_5–Bi_2O_3 glasses by both the SBQ and CBQ techniques are shown in Fig. 1. The X-ray diffractograms of the crystalline V_2O_5 and Bi_2O_3 are also shown in Fig. 1 (Curves a and b) for comparison. In case of V_2O_5, several peaks are observed, out of which the peaks at 2θ = 15.4°, 20.3°, 21.7°, 26.2°, 31.0°, 32.4°, 33.4°, 41.3°, 45.5°, 37.3°, 48.9°, 51.2°, 52.0°, 61.2° and 62.1° are quite sharp and strong. In case of Bi_2O_3, sharp and strong peaks are observed at 2θ = 19.8°, 21.9°, 25.9°, 27.5°, 33.4°, 35.2°, 37.0°, 46.4°, 52.5°, 54.9° and 56.0°. Curves (c) to (i) of Fig. 1 show that good amorphous structures are observed in the samples with 95 to 75 mol % V_2O_5 prepared by the SBQ technique. Good amorphous structures are also observed in the samples with 95 to 70 mol % V_2O_5 prepared by the CBQ technique. For the samples prepared by the SBQ technique with V_2O_5 content 70 mol % or less, weak crystalline peaks are observed. Similarly, the samples obtained by CBQ technique with V_2O_5 content less than 70 mol % show crystalline structures. Curve (k) of Fig. 1 shows that with 65 mol % V_2O_5 (CBQ), weak crystalline peaks are observed at 2θ = 19.0°, 29.0°, 30.6°, 34.6°, etc.

Curves (i) and (j) of Fig. 1 show the X-ray diffractograms of the sample with 80 mol % V_2O_5 after annealing at 200° C for 2 h and after a second heat-treatment at 255° C for 2 h respectively. It may be observed that the sample remains amorphous after annealing at 200° C, but crystalline structures develop during the second heat-treatment at 255° C. Similar effects have also been observed in other compositions of the glasses. This has also been confirmed by the SEM pictured discussed later in the text.

3.2. Infrared spectra (IR) and structural investigations

The room-temperature infrared spectra in the region 200 to 4000 $\mathrm{cm^{-1}}$ of all the V_2O_5–Bi_2O_3 glass samples containing 95 to 70 mol % V_2O_5 in KBr matrix are shown in Fig. 2. For comparison, the spectra of the

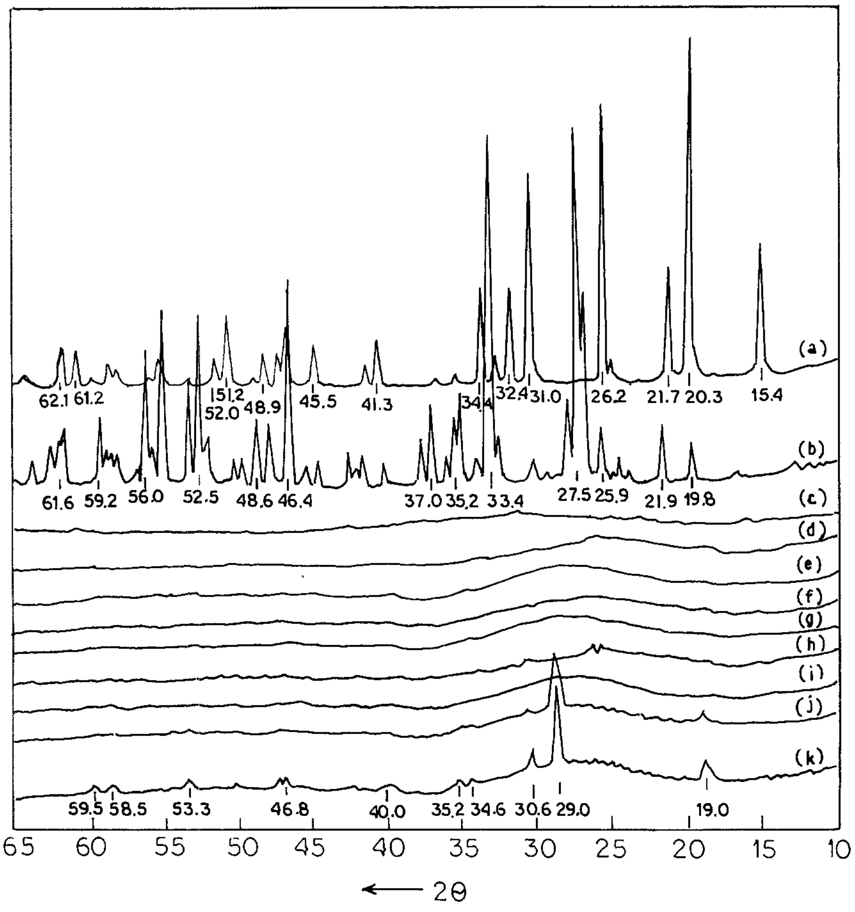

Figure 1 X-ray diffractograms of the V_2O_5–Bi_2O_3 glasses: (a) crystalline V_2O_5, (b) crystalline Bi_2O_3, (c) 95 mol % V_2O_5 (SBQ), (d) 80 mol % V_2O_5 (SBQ), (e) 80 mol % V_2O_5 (CBQ), (f) 75 mol % V_2O_5 (CBQ), (g) 70 mol % V_2O_5 (CBQ), (h) 70 mol % V_2O_5 (SBQ), (i) 80 mol % V_2O_5 (CBQ) annealed at 200° C for 2 h, (j) 80 mol % V_2O_5 (CBQ) second heat-treated at 255° C for 2 h (k) 65 mol % V_2O_5 (CBQ).

crystalline V_2O_5 and Bi_2O_3 are also shown in Fig. 2. The major absorption bands of all the samples are summarized in Table I. The region below 300 cm^{-1} for all the samples did not show any sensitivity possibly due to excessive noise and hence this region has been excluded from the discussion. Both SBQ and CBQ type glasses gave identical spectral character.

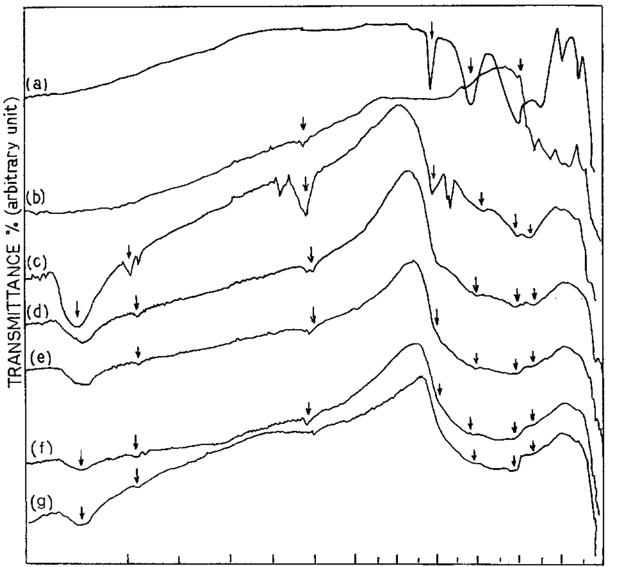

Figure 2 Infrared absorption spectra of the V_2O_5–Bi_2O_3 glasses (CBQ) at room temperature: (a) crystalline V_2O_5, (b) crystalline Bi_2O_3, (c) 95 mol % V_2O_5, (d) 90 mol % V_2O_5, (e) 85 mol % V_2O_5, (f) 80 mol % V_2O_5, (g) 70 mol % V_2O_5.

3.2.1. Crystalline V_2O_5

No water bands or –OH stretching modes are observed in the IR spectrum of the crystalline V_2O_5. Various peaks have been recorded at 1640, 1030, 840, 810, 610, 495, 400 and 320 cm^{-1}. Rivoallen *et al.* [19] have reported an IR spectrum of vitreous V_2O_5 having peak positions at 1020, 810, 600 and 480 cm^{-1}. These authors also found that the peak positions remained unaffected, and only the sharpness changed because of the change of the crystalline to the amorphous phase of V_2O_5. Our data for the crystalline V_2O_5 are in good agreement with those reported by Rivoallen *et al.* [19].

3.2.2. Crystalline Bi_2O_3

Similar to V_2O_5, no water bands are observed in the IR spectrum of Bi_2O_3 (Curve b, Fig. 2). The absorption peaks at 1400, 610, 525, 450, 395 and 360 cm^{-1} have been recorded for this material.

3.2.3. Main features in the IR spectra of various glasses

(a) All the glass samples exhibited a water band at ~ 3400 cm^{-1} and an –OH stretching peak at 2920 cm^{-1}. These peaks become intense in the glasses containing a lower V_2O_5 content. However, the peak position shifted slightly towards the longer wavelength as the content of V_2O_5 decreased. According to Borrellie *et al.* [20] and Quan and Adams [21], these peaks may be due to the hygroscopic character of the powdered glass samples.

(b) An absorption peak at 1640 cm^{-1} was observed for all the glasses. The intensity of the peak decreased as the V_2O_5 content decreased. The origin of this peak is not obvious, but the –OH bending mode may give

TABLE I Positions of peaks in the infrared absorption spectra of V_2O_5–Bi_2O_3 glasses (CBQ) at room temperature

Composition (mol %)		Absorption peak positions (cm^{-1})									
V_2O_5	Bi_2O_3										
100	0				1030	840	610		495	400	320
95	5	3460	2960	1640	1030		610	525			320
90	10	3400	2920	1630	1020		610	525			320
85	15	3400	2920	1640	1020		610	525			320
80	20	3440	2920	1640	1020		610	525			320
75	25	3440	2960	1440	1020		610	525			320
70	30	3440	2920	1440	1020		610	525			320
0	100		1600	1480	1400	870	610	525	450	395	360

rise to absorption in this region and the possibility of absorbed water giving rise to these peaks cannot be ruled out.

(c) An absorption peak at ~ 1030 cm^{-1} was observed for 95 mol % V_2O_5 content. The frequency of this peak decreased slightly to 1020 cm^{-1} as the V_2O_5 content decreased from 95 to 85 mol % and became a shoulder as the V_2O_5 content decreased to 70 mol %.

It has been reported that the V^{5+} ion exists in six-fold coordination in crystalline V_2O_5 [22]. It has also been recognized [23] that as long as the coordination of a cation remains constant, the infrared spectra of the samples of a given compound are similar. If the compositions of V_2O_5 in the glassy state and in the crystalline state give rise to similar absorption bands corresponding to that of the V–O bond vibration in crystalline V_2O_5, it would indicate that the V^{5+} ions in the glassy state are also in six-fold coordination. Dachille and Roy reported [23] that the peak at 1020 cm^{-1} of the crystalline V_2O_5 is due to the vanadium–oxygen stretching frequency; they also observed that the vanadium–oxygen stretching frequency for compounds in which the vanadium atoms are totally ionized to V^{5+}, is in the range 1025 to 1005 cm^{-1}, and that the presence of V^{4+} ions appears to reduce the vanadium–oxygen stretching frequency in the range 900 to 1025 cm^{-1}. From these data, and comparing the vibrational spectra of V_2O_5 in the crystalline state and of V_2O_5–Bi_2O_3 in the glassy state, one can conclude that the peak at 1020 cm^{-1} in the glasses is due to V–O stretching frequency. In addition the IR spectrum of crystalline Bi_2O_3 shows no peak at 1020 cm^{-1} and this confirms that the peak at 1020 cm^{-1} is associated with the V–O stretching frequency. From Fig. 2, it is obvious that the normal vibrational frequency of the V–O bond seen in crystalline V_2O_5 content decreases. This can be seen in all the spectra of the glass samples, indicating that the V^{5+} ions exist in six-fold coordination in the glasses as well as in the crystalline V_2O_5.

(d) A vibrational peak at 525 cm^{-1}, observed in crystalline Bi_2O_3, was retained in all the glass samples, although the intensity of the peak decreased gradually as the V_2O_5 content decreased. This peak at 525 cm^{-1} was not observed in the crystalline V_2O_5.

(e) The peak at 610 cm^{-1}, which was observed in crystalline V_2O_5 and Bi_2O_3, was also observed in all the glass samples. The intensity of the peak decreased gradually below 90 mol % V_2O_5.

(f) An absorption peak at 840 cm^{-1}, observed in crystalline V_2O_5, disappeared in all the glass samples. Also the peaks at 495 and 400 cm^{-1}, observed in crystalline V_2O_5 and at 1400, 450 and 395 cm^{-1}, in crystalline Bi_2O_3, disappeared completely in the glass samples. Rivoallen *et al.* [19] reported that no marked change in the absorption frequencies of the crystalline and amorphous phase of V_2O_5 occurred. Therefore, the absence of these peaks indicates that either the structural units of V_2O_5 in the V_2O_5–Bi_2O_3 glasses are not the same as that in the amorphous V_2O_5, or the intensity of the peaks becomes too weak to be detected.

3.3. Chemical compositions

The analysed compositions of the glasses and the estimated concentrations of V^{4+} and total vanadium ions (N) are shown in Table II. The analysed compositions are slightly different from the batch compositions due to evaporation losses during melting. The ratio (C) of the concentration of V^{4+} ions to the concentration of total vanadium ions (shown in Table II) decreases with the increasing concentration of V_2O_5 in the glasses. Assuming the vanadium ions to be uniformly distributed in the glass matrix, the average (V–V) site spacing, R, has been calculated from the total

TABLE II Chemical composition, concentration of V^{4+} and total vanadium ions, glass transition temperature, density and average site spacing of V_2O_5–Bi_2O_3 glasses

Starting composition (mol % V_2O_5)	Final composition (mol % V_2O_5)	N (10^{22} cm^{-3})	V^{4+} (10^{20} cm^{-3})	V^{4+} (10^{20} cm^{-3})*	$C = \frac{V^{4+}}{V_{total}}$	T_g (°C)	Density ($g\,cm^{-3}$)	R (nm)
70	70.8	2.05	7.88	7.69	0.026	265 ± 5	3.49	0.365
75	75.6	2.12	4.86	4.50	0.023	265 ± 5	3.40	0.361
80	80.5	2.20	4.32	4.21	0.020	262 ± 5	3.32	0.357
85	85.5	2.25	4.17	4.00	0.019	263 ± 5	3.26	0.354
90	90.3	2.28	4.01	3.96	0.017	260 ± 5	3.17	0.352
95	95.2	2.34	3.81	3.75	0.016	260 ± 5	3.02	0.349

*From EPR measurements.

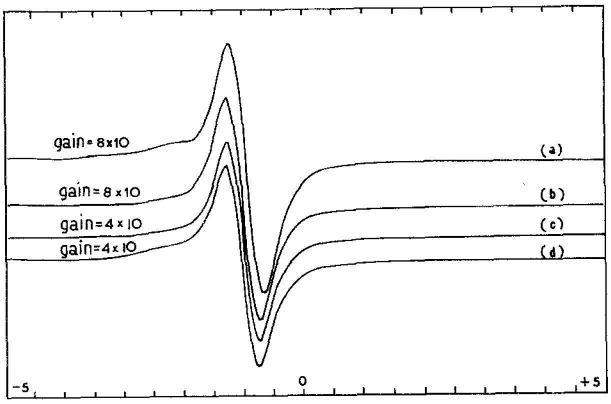

Figure 3 EPR spectra of some V_2O_5–Bi_2O_3 glasses (CBQ): (a) 70 mol % V_2O_5 at 300 K, (b) 80 mol % V_2O_5 at 300 K, (c) 90 mol % V_2O_5 at 300 K, (d) 80 mol % V_2O_5 at 80 K. Scan range 8 kG, field set 4000 G. Time constant 1 sec, scan time 4 min. Modulation amplitude 4 × 10 G, modulation frequency 100 kHz. Microwave power 20 mW, microwave frequency 9.15 GHz.

vanadium ion concentration and are shown in Table II. Table II shows that the value of *R* decreases with the increase of V_2O_5 content in the glasses. No difference has been noticed in the chemical compositions of the SBQ and CBQ glasses.

3.4. EPR spectra

The EPR spectra of some samples at room temperatures of 300 and 80 K are shown in Fig. 3. For all the glasses the EPR spectra appear as a single line which means that the reduced valence states, below the first reduced state (V^{4+}), are negligible. It may also be noted that the line shapes of the spectra are the same for the two temperatures. This indicates that the spin concentrations (V^{4+}) are almost independent of temperature and that there is no thermally generated carriers in these glasses.

The concentrations of V^{4+} ions as determined from these spectra are shown in Table II. The values of V^{4+} concentrations agree well with the results of the chemical analysis within the experimental error (Table II).

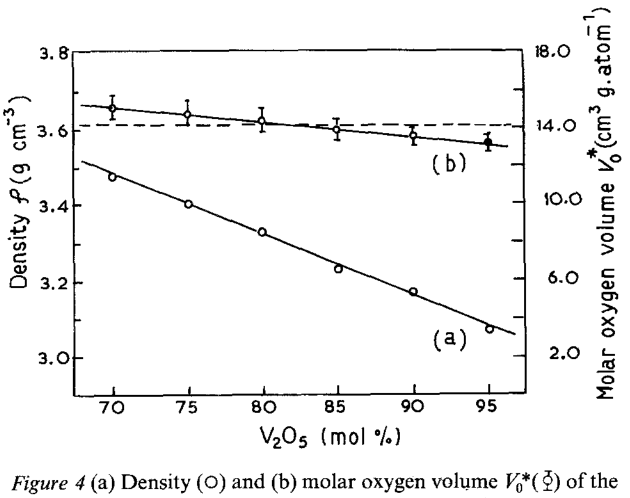

Figure 4 (a) Density (○) and (b) molar oxygen volume V_0^*(⧲) of the V_2O_5–Bi_2O_3 glasses (CBQ) as a function of the concentration of V_2O_5; (---) arithmetic mean; vertical lines, estimated experimental uncertainty.

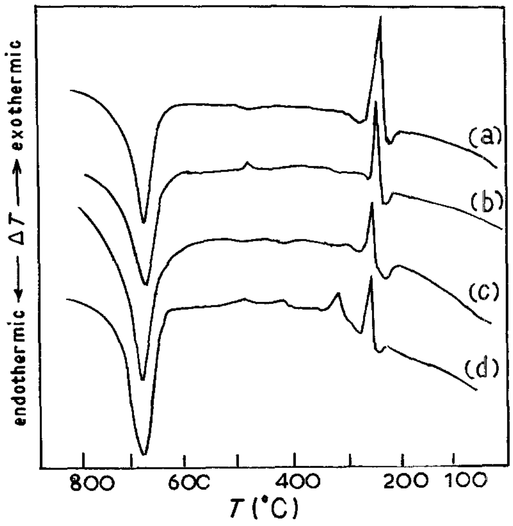

Figure 5 DTA curves of the V_2O_5–Bi_2O_3 glasses; (a) 90 mol % V_2O_5 (CBQ), (b) 80 mol % V_2O_5 (CBQ), (c) 70 mol % V_2O_5 (CBQ), (d) 80 mol % V_2O_5 (SBQ).

3.5. Density and apparent molar volume of oxygen

The density of the glass samples is shown in Fig. 4 as a function of the concentration of V_2O_5 in the glasses. It is observed that the density decreases almost linearly with increasing V_2O_5 content in the glasses.

It is frequently revealing to express the relationship between the density of an oxide glass and its composition in terms of the apparent volume, V_0^*, occupied by 1 g atom O_2. The values of V_0^* for the V_2O_5–Bi_2O_3 glasses have been calculated from the formula given by Drake *et al.* [24] and are shown in Fig. 4 as a function of compositions of the glasses. The mean value of V_0^* is 14.2 cm^3 g atom^{-1} and the standard deviation 0.03 cm^3 g atom^{-1} is approximately equal to the estimated experimental uncertainty. Fig. 4 shows that V_0^* changes linearly with composition, suggesting that the glasses appear to be in a single phase with random structure, and that the geometry and topology of the random network remain unchanged with composition [24]. No composition-dependent structural changes or phase separations have occurred in the glasses.

3.6. Glass transition temperatures

The glass transition temperatures (T_g) of the glasses were determined from the DTA curve shown in Fig. 5 and are shown in Table II. The T_g of the glasses lie in the range 260 to 270° C and are found to be greater than T_g (216° C) of the amorphous V_2O_5 [19]. T_g increases with the decrease of V_2O_5 content in the glasses and is found to be sensitive to the preparation conditions. Fig. 5 also shows that the T_g, as well as the nature of the DTA curves of the samples obtained by SBQ and CBQ techniques, are slightly different. This difference also reflects from the electrical conductivity discussed below.

3.7. Thermal annealing and microstructure

The microstructures of the glasses before and after annealing at different temperatures have been investigated by scanning electron microscopy (SEM). Fig. 6

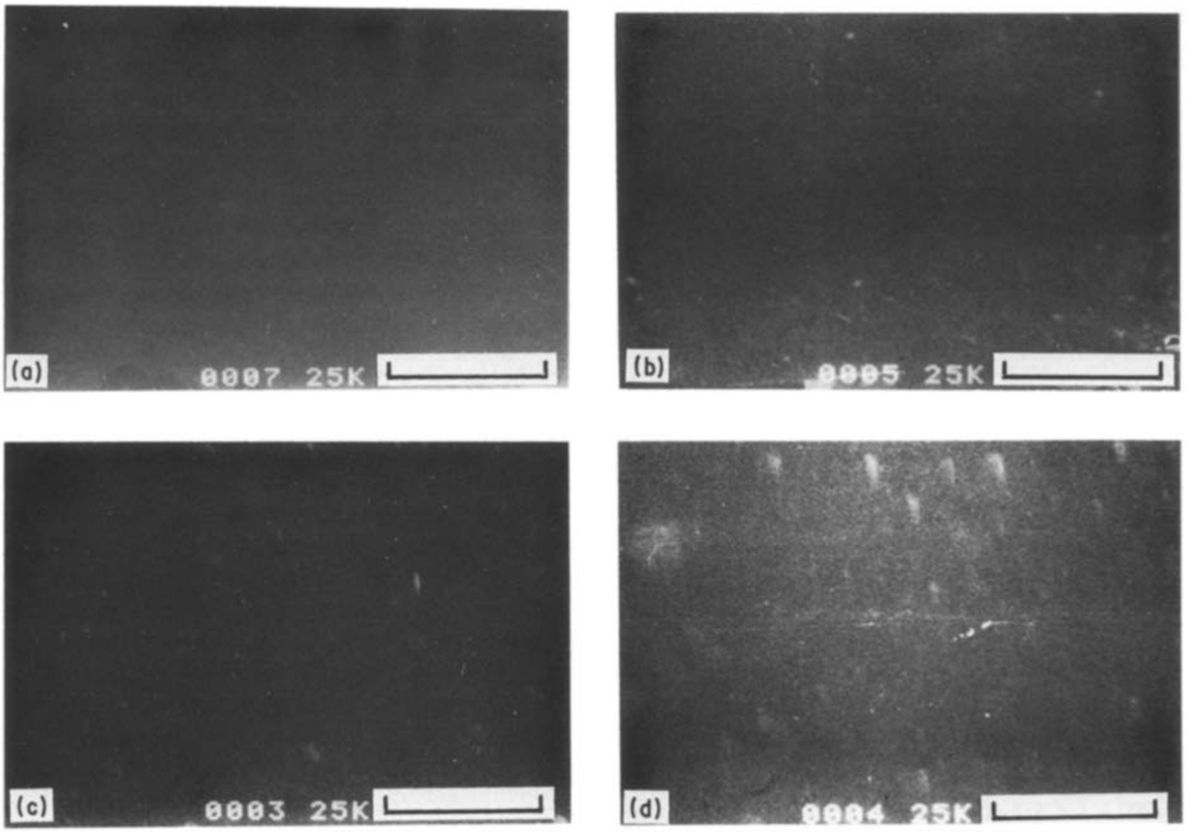

Figure 6 Scanning electron micrographs of some $80V_2O_5$–$20Bi_2O_3$ glass (CBQ): (a) annealed at 200° C for 2 h, (b) after second heat-treatment at 255° C for 1 h, (c) after second heat-treatment at 255° C for 2 h, (d) after second heat-treatment at 255° C for 16 h. Scale bars: (a–c) 10 μm; (d) 30 μm.

shows scanning electron micrographs of some samples before and after annealing at 200° C and also after the second heat-treatment at 255° C for different durations of time. It may be observed that annealing of the $80V_2O_5$–$20Bi_2O_3$ glass up to 200° C did not induce any crystallinity in the glass, but the crystalline phases develop during the second heat-treatment at 255° C and become prominent with the increasing heating time. Similar results are also observed in other glass compositions. Chung and Mackenzie [25] have noticed a crystalline phase in V_2O_5–TeO_2 glasses after heat-treatment at $\sim 270°$ C and have identified this crystalline phase to be close to the V_4O_9 phase [26]. No difference has been detected in the scanning electron micrographs of SBQ and CBQ samples.

3.8. D.c. conductivity ($\sigma_{\mathrm{d.c.}}$)

The logarithm of d.c. conductivity of the glass samples (CBQ) plotted against mol % V_2O_5 at 300 K is shown in Fig. 7. For comparison, the data for V_2O_5–P_2O_5 [7] and V_2O_5–TeO_2 glasses [9] are also plotted in the same figure. It is noted that the conductivity increases with increasing V_2O_5 content in the glasses. A general trend of different glass formers is that $\sigma_{TeO_2} > \sigma_{P_2O_5} > \sigma_{Bi_2O_3}$. However, the difference is well within a factor of three.

The log d.c. conductivity–$10^3/T$ plot is shown in Fig. 8 showing increasing conductivity with increasing temperature. In the investigated temperature region, no marked dependence of the activation energy on temperature has been observed. This observation is also consistent with the reported data for V_2O_5–P_2O_5 [7] and V_2O_5–TeO_2 [9] glasses. In these glasses a temperature-dependent activation energy is observed below 200 K. Detailed studies of low-temperature conductivity and activation energy of the V_2O_5–Bi_2O_3 glasses containing 80 to 95 mol % V_2O_5 have been reported earlier [27].

It is seen from Fig. 8 that the conductivity of the same sample obtained by different quenching techniques is different. For example, with 80 mol % V_2O_5, the conductivity of glasses obtained by CBQ is larger than that of the glasses obtained by SBQ. This is expected because of the difference in the thermal history of the samples prepared by these two techniques. It is also noted that the conductivity of the

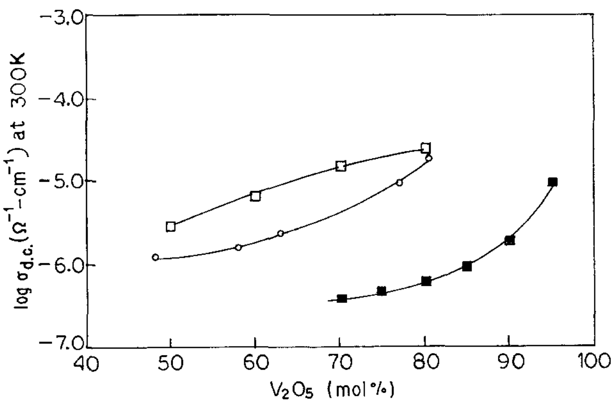

Figure 7 D.c. conductivity plotted against mol % V_2O_5 for (■) V_2O_5–Bi_2O_3 glasses (CBQ), (□) V_2O_5–P_2O_5 glasses [7] and (○) V_2O_5–TeO_2 glasses [9].

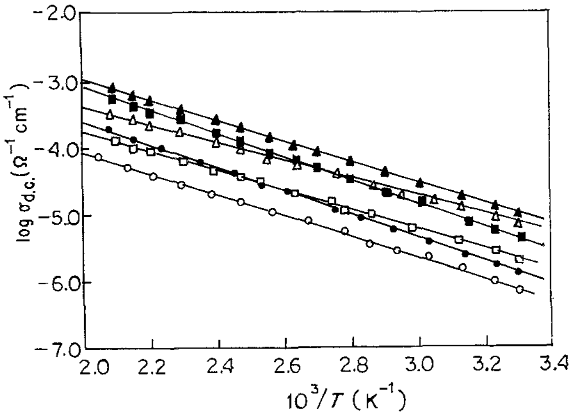

Figure 8 Variation of d.c. conductivity with $10^3/T$ for the V_2O_5–Bi_2O_3 glasses: (○) 70 mol % V_2O_5 (CBQ) annealed at 200° C for 2 h; (●) 80 mol % V_2O_5 (CBQ) annealed at 200° C for 2 h; (□) 90 mol % V_2O_5 (SBQ) annealed at 200° C for 2 h (■) 80 mol % V_2O_5 (CBQ) after second heat-treatment at 255° C for 2 h (△) 90 mol % V_2O_5 (CBQ) annealed at 200° C for 2 h; (▲) 95 mol % V_2O_5 (CBQ) annealed at 200° C for 2 h.

second heat-treated glasses at 255° C is larger than that of the glasses annealed at 200° C. A larger increase of conductivity of the second heat-treated glasses, compared to that of the glasses annealed at 200° C, has been observed at low temperatures [27]. This larger conductivity is due to the development of a crystalline structure in the second heat-treated glasses at 255° C as evinced by scanning electron micrographs.

A plot of d.c. conductivity against activation energy for the V_2O_5–Bi_2O_3 glasses is shown in Fig. 9 at $T = 300\,K$. For comparison the data for V_2O_5–P_2O_5 [7] and V_2O_5–TeO_2 glasses [9] have also been included. It is seen from Fig. 9 that the activation energy decreases with increasing conductivity. The slope of the curve for V_2O_5–Bi_2O_3 glasses gives $T = 330\,K$ which is comparable to the temperature (300 K) for which the data have been taken. As suggested by Murawski *et al.* [6], this indicates that the high-temperature conduction mechanism in the V_2O_5–Bi_2O_3 glasses is the adiabatic hopping of polarons similar to V_2O_5–P_2O_5 glasses [7].

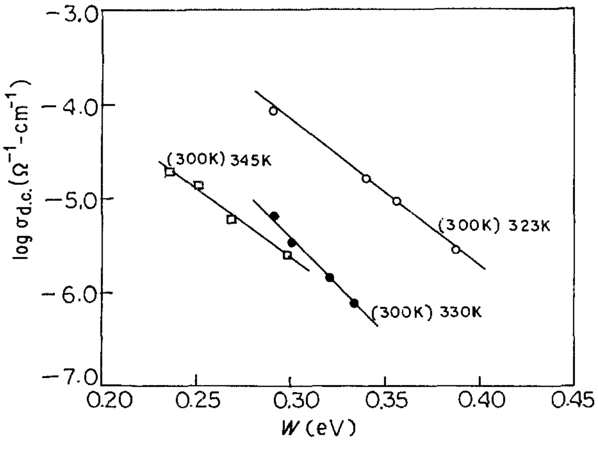

Figure 9 Variation of d.c. conductivity with activation energy: (●) V_2O_5–Bi_2O_3 glasses (CBQ); (○), V_2O_5–P_2O_5 [7]; (□) V_2O_5–TeO_2 [9] glasses. The values in parentheses are the experimental temperatures, the other values correspond to the slope.

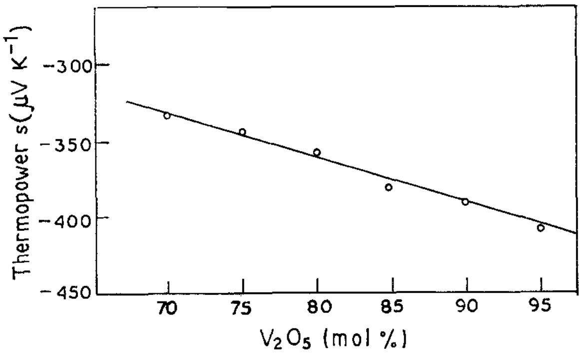

Figure 10 Composition dependence of the thermopower at 400 K.

3.9. Thermopower

In the investigated temperature range (300 to 500 K), the thermopower of the V_2O_5–Bi_2O_3 glasses (SBQ or CBQ) is found to be independent of temperature. The sign of the thermopower is always negative for all the glass compositions indicating that the charge carriers are electrons or polarons. The composition dependence of the thermopower at 400 K is shown in Fig. 10. It may be observed that the magnitude of the thermopower increases with increasing V_2O_5 content in the glasses.

The temperature-independent thermopower of transition metal oxide glasses is fitted with Heikes' relationship [28]

$$S = (k_B/e)\{\ln[C/(1 - C)] + \alpha'\} \quad (1)$$

where C is the ratio of the concentration of reduced transition metal ion to the concentration of the total transition metal ions, $\alpha' k_B T$ is the kinetic energy of a carrier. The value of α' needed in Equation 1 to make a complete agreement between the experimental value and that given by Equation 1 is in the range 0.13 to 0.51 depending on compositions of the glasses. This value of α' signifies the formation of small polarons in the V_2O_5–Bi_2O_3 glasses as suggested by Austin and Mott [4].

4. Conclusions

The X-ray data reveal that stable glasses in the system V_2O_5–Bi_2O_3 are obtained in the composition range 95 to 70 mol % V_2O_5. Crystalline structures are observed in the samples containing less than 70 mol % V_2O_5. The infrared spectra of the glasses suggest that the fundamental vibrational frequency of the V–O bond occurs at $1020\,cm^{-1}$ and the V^{5+} ions exist in six-fold coordination as in crystalline V_2O_5. Some bands, characteristics of crystalline V_2O_5 and Bi_2O_3, disappear in the glasses. The glasses appear to be in a single phase, and the geometry and topology of the structure do not change with glass compositions. The average (V–V) site spacing decreases with the increasing V_2O_5 content in the glasses. EPR spectra show that the spin concentration is almost independent of temperature and there are no thermally generated carriers in these glasses. The samples remain amorphous after annealing at 200° C for 2 h, but crystalline structures develop in the samples during a second heat-treatment at 255° C.

The electrical and thermal (DTA) properties of the V_2O_5–Bi_2O_3 glasses are sensitive to the thermal history of preparations, unlike other properties studied. The d.c. conductivity increases with increasing V_2O_5 in the glasses. In the investigated temperature range (300 to 500 K), the activation energy is almost independent of temperature and the electrical conduction is due to adiabatic hopping of polarons in the glasses. The thermopower is independent of temperature and increases with increasing V_2O_5 content in the glasses. Thermopower also provides evidence for small polaron formation in the V_2O_5–Bi_2O_3 glasses.

Acknowledgements

The authors are grateful to Professor C. K. Majumdar, Head of the Magnetism Department, I.A.C.S. for his interest in the work. The authors also thank Dr D. K. Nag of G.S.I. for his help in taking X-ray diffraction and Dr S. K. Brahma of the Department of Chemistry, Jadavpur University for his help in discussing IR spectra. Thanks are also due to Dr S. K. Gupta, EPR Section, NPL for his help in taking EPR spectra.

References

1. E. P. DENTON, H. RAWSON and J. E. STANDWORTH, *Nature.* **173** (1954) 1030.
2. J. D. MACKENZIE, "Modern Aspects of Vitreous State", Vol. 3 (Butterworth, Washington, 1964) p. 126.
3. C. H. CHUNG, J. D. MACKENZIE and L. MURAWSKI, *Rev. Chim. Miner.* **16** (1979) 308.
4. I. G. AUSTIN and N. F. MOTT, *Adv. Phys.* **18** (1969) 41.
5. I. G. AUSTIN and E. S. GARBETT, "Electronic and Structural Properties of Amorphous Semiconductors", (Academic, New York, 1973) p. 393.
6. L. MURAWSKI, C. H. CHUNG and J. D. MACKENZIE, *J. Non-cryst. Solids* **32** (1979) 91.
7. M. SAYER and A. MANSINGH, *Phys. Rev.* **B6** (1972) 4629.
8. G. S. LINSLEY, A. E. OWEN and F. M. HAYATEE, *J. Non-cryst. Solids* **4** (1970) 208.
9. V. K. DHAWAN, A. MANSINGH and M. SAYER, *ibid.* **51** (1982) 87.
10. K. W. HANSEN and M. T. SPLANN, *J. Electrochem. Soc.* **113** (1966) 895.
11. M. SAYER and A. MANSINGH, *J. Non-cryst. Solids* **31** (1979) 385.
12. G. W. ANDERSON and W. D. COMPTON, *J. Chem. Phys.* **52** (1970) 6166.
13. A. K. BANDYOPADHYAY, J. O. ISARD and S. PARKE, *J. Phys. D. Appl. Phys.* **11** (1978) 2559.
14. A. PAUL and N. YEE, *J. Non-cryst. Solids* **24** (1977) 259.
15. L. D. BOGOMOLOVA, T. F. DOLGOLENKO, V. N. LAZUKIN and I. V. FILALOVA, *J. Sov. Phys. Sol. Stat.* **15** (1974) 2477.
16. A. K. BANDYOPADHYAY, *J. Mater. Sci.* **16** (1981) 189.
17. M. S. R. HEYNES and H. RAWSON, *J. Soc. Glass Technol.* **41** (1957) 347T.
18. Y. KAWAMATO, M. FUKUZUKO, Y. OHTA and M. IMAI, *Phys. Chem. Glasses* **20** (1979) 54.
19. L. RIVOALLEN, A. REVCOLEVSCHI, J. LIVAGE and R. COLLONGNES, *J. Non-cryst. Solids* **21** (1976) 171.
20. N. F. BORRELLI, B. D. McSWAIN and GOUG-JEN SU, *Phys. Chem. Glasses* **4** (1963) 11.
21. J. T. QUAN and C. F. ADAMS, *J. Phys. Chem.* **70** (1966) 331.
22. B. H. V. JANAKIRAMA-RAO, *J. Amer. Ceram. Soc.* **49** (1966) 605.
23. E. DACHILLE and R. ROY, *ibid.* **42** (1965) 78.
24. C. F. DRAKE, J. A. STEPHENS and B. YATES, *J. Non-cryst. Solids* **28** (1978) 61.
25. C. H. CHUNG and J. D. MACKENZIE, *ibid.* **42** (1980) 357.
26. G. GRYMONPREZ and J. VEHNIK, *Acta Crystallogr.* **A33** (1977) 834.
27. A. GHOSH and B. K. CHAUDHURI, *J. Non-cryst. Solids* **83** (1986) 151.
28. R. R. HEIKES and R. W. URE, "Thermoelectricity" (Interscience, New York, 1961) p. 81.

Received 24 June
and accepted 3 December 1986